UCID- 16986-89-1

LAWRENCE LIVERMORE NATIONAL LABORATORY

OIL SHALE QUARTERLY REPORT

January - March 1989

EDITED BY

Robert J. Cena

May 1989

Lawrence
Livermore
National
Laboratory

Work performed under the auspices of the U.S. Department of Energy by the Lawrence Livermore National Laboratory under Contract W-7405-Eng-48.

Price Code	Page Range
A01	Microfiche
Papercopy Prices	
A02	001–050
A03	051–100
A04	101–200
A05	201–300
A06	301–400
A07	401–500
A08	501–600
A09	601

<u>TABLE OF CONTENTS</u>

ISOTHERMAL PYROYSIS KINETICS

Obtaining accurate kinetics of oil generation and associated oil degradation reactions is an important part of understanding and improving oil shale pyrolysis processes. While programmed micropyrolysis at several heating rates offers one method for measuring chemical kinetics data, an alternative method that is rapid and potentially more accurate (e.g., in relating the kinetics to a specific temperature or temperature range) is the use of an isothermal fluidized bed. A principal hindrance in interpreting fluidized-bed data is that the signal being measured can undergo significant delay and dispersion from the time it is generated until it reaches the detector. The measured reaction rate can be significantly different from the true rate. Meaningless kinetic parameters can be obtained by ignoring those differences. A tracer signal measured under the same conditions will help quantify the dispersion. Mathematically, the measured rate can be expressed as the convolution of the true rate and the tracer:

$$h(\tau) = \int_{-\infty}^{\infty} f(t)\, g(\tau - t)\, dt,$$

where f is the true reaction rate, g is the measured tracer pulse, and h is the measured reaction rate. Deconvolution procedures can be used to obtain the true reaction rate. We have, however, found that the noise in the results is often unacceptable. An alternative procedure, when comparing measured rates with theoretically calculated rates, is to convolute the calculated rates with the tracer. In a least-squares program for determining reaction rate parameters, the disadvantage is that the convolution must be done numerous times. The advantage, however, is that essentially noise-free results are obtained.

We have modified our kinetics analysis program, KINETICS, to make use of tracer data by means of the latter procedure. During the course of the least-squares refinement of the reaction rate parameters, the tracer is convoluted with the theoretically calculated reaction rates as:

$$h_c(j) = \sum_{i = j - n_2 + 1}^{j - n_1 + 1} f_c(i)\, g(j - i + 1),$$

where f_c is the theoretically calculated reaction rate, h_c is the convoluted calculated rate, n_1 is the first nonzero point in the tracer pulse, and n_2 is the last nonzero point in the tracer pulse. The tracer supplied to KINETICS must be either a pulse (rate data) or a step (integral data). It cannot be a square wave. The tracer data can be on a relative scale and must be supplied for each experiment in the set being analyzed. A further requirement is that the reaction rate data and the tracer data be measured with a constant time interval for a given experiment.

This tracer method was applied to the analysis of data from fluidized-bed pyrolysis of Anvil Points 24-gpt (AP24) shale at 450, 475, 500, and 525°C The approximate temperature of the shale during the initial heatup was calculated using a time constant of 0.5 second. First, the analysis of the shale data was done without the use of tracer data and very poor results were obtained. The principal activation energy was less than 40 kcal/mol, compared with the expected value of 51 to 52 kcal/mol determined by nonisothermal methods using programmed micropyrolysis at several heating rates. Much better results were obtained when tracer data were used. The tracer data were obtained at each of the shale temperatures by fluidized-bed pyrolysis of firebrick impregnated with C-18. The detector response at each temperature is shown in Figure 1. Simultaneous analysis of all four AP24 experiments, using the tracer measured at the corresponding shale temperature gave the results shown in the first column of Table 1. In all of these analyses, the data were modelled in terms of two parallel reactions, with the constraint that A1 = A2. The fractions reacting by each reaction are shown as f_1 and f_2. While the principal activation energy of 47.9 kcal/mol is closer to the expected value than we had obtained for the nontracer analysis, it is still too low.

Inspection of the tracer data revealed possible problems at 525°C. The tracer profiles at 450, 475, and 500°C were essentially superimposable, whereas the profile at 525°C was significantly different (see Figure 1). We repeated the kinetic analysis applying the tracer data at 500°C to all four experiments. The results reported in column two of Table 1 show excellent agreement in activation energy with nonisothermal kinetic data with the principal activation energy being 51.0 kcal/mol. Comparison of data and fit at the four temperatures are shown in Figure 2.

In conclusion, the tracer method used here appears to be a viable method for obtaining shale pyrolysis kinetics from fluidized-bed experiments. Moreover, for a given fluidization velocity and equipment configuration, it may be necessary to measure the tracer pulse only at one temperature in the range of shale temperatures being studied. The tracer profile, however, should be measured in duplicate to assure its precision. It is also important to carefully select a consistent zero time for the shale data and the tracer data. Since this can be done, at best, to within one time interval, a relatively small time interval must be used. For shale pyrolysis up to 525°C, the time interval should be one second or less.

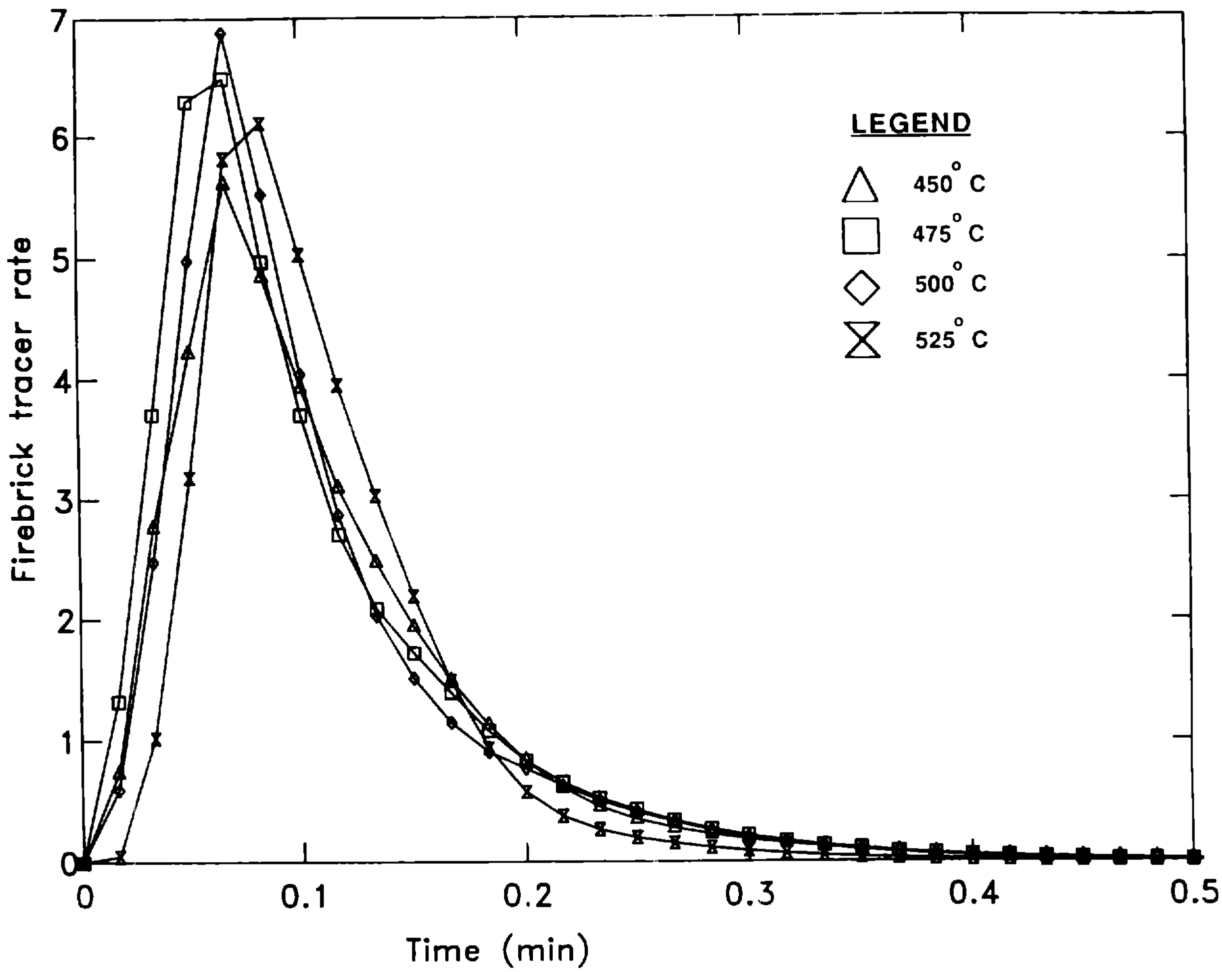

Figure 1. Firebrick impregnated C-18 tracer responce at four temperatures.

Table 1. Kinetics analysis of AP24 data from fluidized-bed pyrolysis at 450, 475, 500, and 525°C.

	Use tracer data at same temperature as shale data	Use tracer data at 500°C for all shale data
A (s^{-1})	2.30×10^{12}	1.92×10^{13}
E_1 (kcal/mol)	40.9	45.0
E_2 (kcal/mol)	47.9	51.0
f_1	0.171	0.157
f_2	0.829	0.843

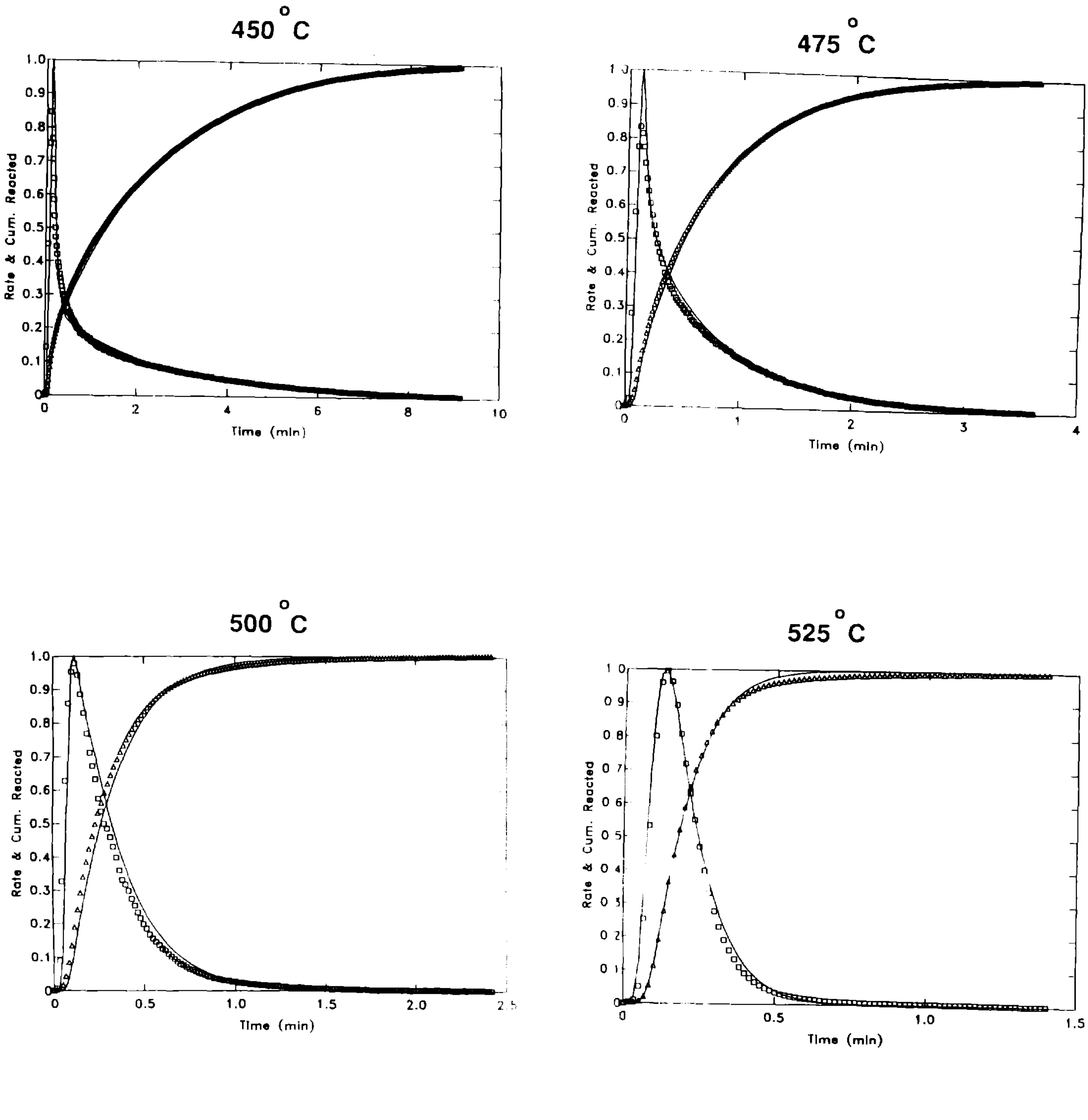

Figure 2. Comparison of pyrolysis data (points) versus kinet fit (line) at four temperatures. Anvis Points 24 gallon-per-ton shale.

DUST

Dust is a common problem in the handling and processing of solids. Above-ground oil-shale processing requires a large number of dust-generating steps. In some retort designs, dust cannot be processed. In other designs dust is transported out of the pyrolyzer before being fully retorted. In either case, dust not retorted can represent a significant oil loss. Dust is troublesome in other ways. It can cause rapid wear and failure of bearings and valves. Dust contributes to the toughness of plugs of heavy oil and coke which sometimes form in pipes carrying oil vapors, and dust provides most of the surface area for coking and cracking of oil vapors.

Separation of oil shale dust from larger particles in process streams is generally accomplished by cyclone separators. The distribution of dust, and other solids, in the LLNL solids-recycle oil shale retort is shown in Table 2 The results from different retorts and three grades of Green River shale are shown.

Table 2
DISTRIBUTION OF PROCESSED SOLIDS, WEIGHT PERCENT
LLNL Solids-Recycle Retorts
Recycle Ratio 4/1

	Fluidized Bed		Packed Bed		
Shale & Grade (gal/ton)	AP24	AP24	OX15	AP24	CB42
Experiment #	R-4	R-7	G-3	G-12	G-14
Location of Solids					
Spent Shale Hopper	59.8	63.7	83.5	62.5	5.3
Pyrolysis Cyclones	36.4	31.0	6.4	20.4	71.5
Combustor cyclones	3.2	4.8	10.0	16.8	22.6
Dust in Oil	0.5	0.5	?	0.2	0.3
Mass balance (solids)					
mass in/mass out	1.02	1.05	1.00	1.04	1.04

Approximately 60% of the raw shale was collected in the spent-shale hopper, both in the case of the fluidized-bed pyrolyzer and the packed-bed pyrolyzer, when a 24 gallon per ton shale from the Anvil Points mine (AP24) was processed. The balance was dust, most of which was collected in the cyclones. In the case of the 42 gallon per ton shale from tract C-b (CB42), all but 5% was worn down to the extent that it was blown into the cyclone separators.

In order to understand the rate of the dust generation during shale processing we have carried out shale attrition esperiments in a laboratory fluidized bed. The bed, and apparatus used to collect dust blown out of the bed, are shown in Figure 3.

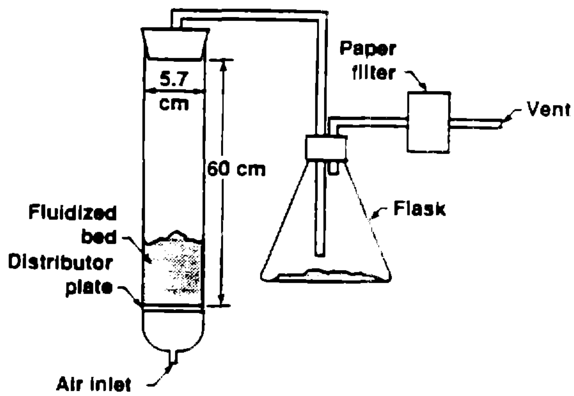

Figure 3. Fluidized bed and dust-collecting apparatus for measurements of shale loss.

The loss of material by the bed, and the amount of material collected in the flask, filter, and the small amount of material in the tubing, were all determined by weighing each component. The mass of shale and dust found at the end of an experiment was 99% or more of the mass of shale at the start of an experiment. Mass loss is shown as a function of time in Figure 4.

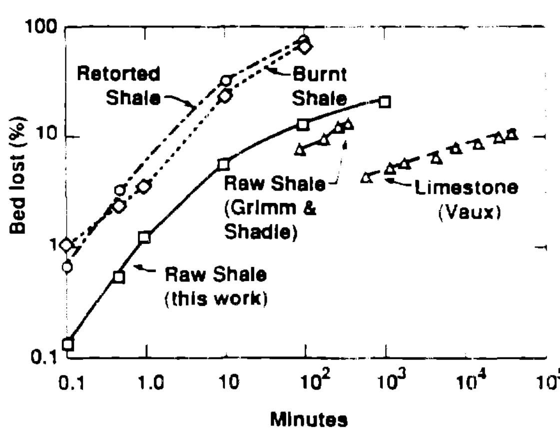

Figure 4. Loss of shale from our laboratory fluidized bed. Data for similar experiments on raw shale (Grimm and Shadle. 1986) and limestone (Vaux, 1978) are included for comparison .

The initial rate of loss of material from raw and processed Green River oil shale was very rapid, and remained more or less constant for the first minute. After the first minute, the rate at which dust was generated and blown out of the fluidized bed decreased approximately a factor of ten for each ten-fold increase in fluidization time.

The amount of burnt or retorted shale blown out of the bed was 5-to 10-times higher than in the case of raw shale. The loss of retorted shale exceeded the loss of burnt shale, when the duration of fluidization was longer than approximately 0.3 min.

With fluidization, particles lost sharp edges and corners, as shown in Figure 5. Processed shale showed the same degree of smoothing as raw shale, but in one tenth the time.

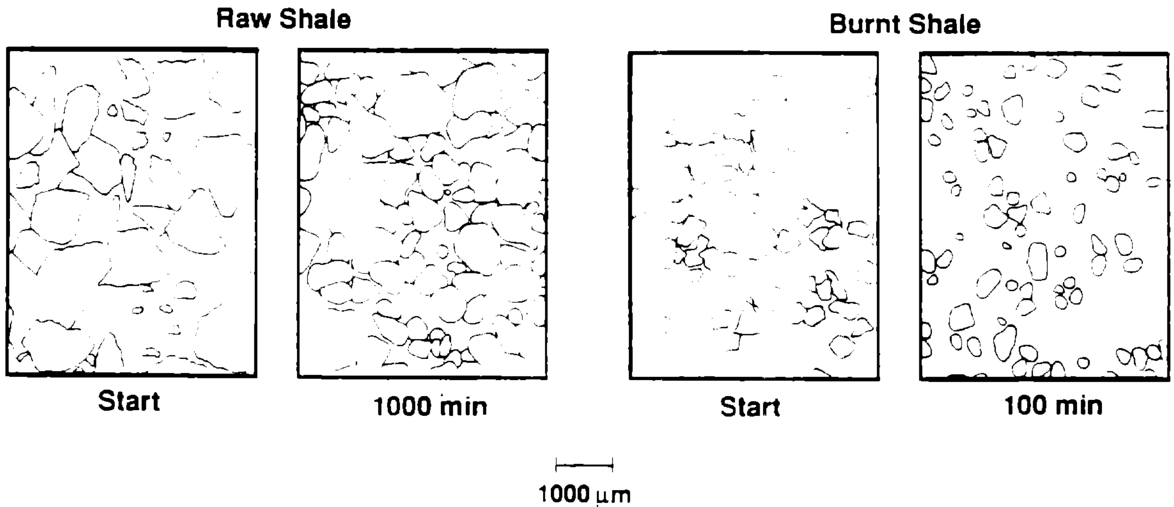

Figure 5. Silhouettes from photographs of raw and burnt shale particles before and after agitation in a flulidized bed. The particles kept the same aspect ratio, but lost sharp corners.

All the dust samples had extremely broad particle-size distributions. The size distributions were bimodal, except for the dust from burned shale. The distribution, after 10 min of fluidization, is given in Figure 4. The distribution did not change much with time.

In the case of raw shale, after an initial period of 100 min, the dust had a distinct bimodal distribution, with a peak in the size range 2-5 µm and a second peak at 60 µm. We ascribed the formation of small particles to wear, and larger particles to fracture. For raw shale the mass of dust of the larger size ranges was dominant, suggesting that fracture was the most important mechanism of bed loss.

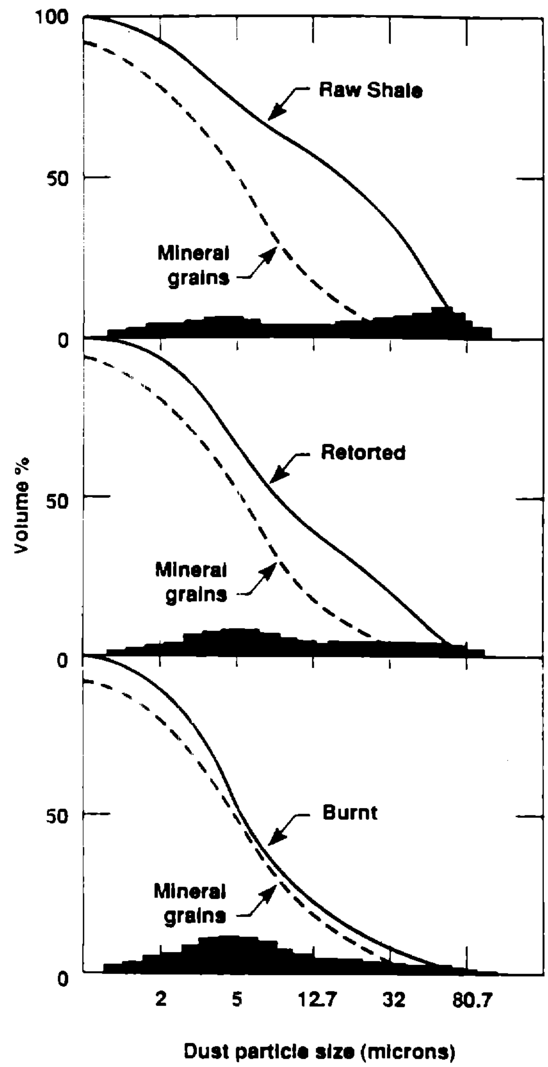

Figure 6. Dust size distribution after 10 min of fluidization. Volume-differential histograms and cumulative curves showing a bimodal distribution of sizes. In the case of dust released by fluidization of burnt shale, the size distribution was close to the size distribution of the individual mineral grains in shale.

We observed that the rate of loss of raw eastern oil shale from a laboratory fluidized bed is much slower than for Green River shale, and the limited data suggests that this shale behaves more like the limestone shown in Figure 4, than Green River shale.

According to theory, particles smaller than 100 µm will be pneumatically conveyed out of the fluidized bed. In fact, we found no particles larger than 150 µm in the attrited material (dust), and few particles smaller than 140 µm in the bed. If particles fractured into halves and then into halves again and again, no very small particles would be seen, for all of these relatively large fragments would be blown out of the bed. Thus a fracture mechanism results in bed loss of material in the 50-100 µm range only, with no fine dust formed.

On the other hand, particle failure can take place by a more gradual wearing away. Wear will tend to yield particles of the smallest structural units in shale, the individual mineral crystals. The size distribution of individual mineral crystals in the shale is shown in Figure 6.

A key question is the application of this laboratory work on small relatively lean shale particles to real systems where the range of grade can be large, and particles 5-10 times larger will be processed.

We imagine that the fraction of shale converted to dust will be less for larger particles because the mass fraction in asperities is less. On the other hand, fluidization and transport velocities will also be higher for larger particles, resulting in much higher energies of collision and shear.

The question of the role of shale grade on attrition is particularly difficult to evaluate. For raw shale, attrition may decrease with increasing grade. However, both in our pilot plant and previous laboratory work, the friability of oxidized rich shale stands out, and the results of the present work cannot be extended to processed rich shale. There can be little doubt that creative new processing techniques will be needed to handle oxidized rich shale.

It would be desirable to be able to make reliable predictions of the amount and size of dust that will be generated by a given shale in a given process based on fundamental physical parameters of shale. It is not clear what properties are the most likely to be useful. Needed are additional measurements of attrition of shales and processed shales of a range of grade and particle sizes, along with measurements of the shear, tensile, and crushing strength for the same shales.

REFERENCES

Grimm, U., and Shadle, L. J., "Size, Mineral, and Organics Distribution in Crushed Oil Shales," Chemical Separations, 2, 199-218.

Vaux, W. G., 1978, "Attrition of Particles in the Bubbling Zone of a Fluidized Bed", Proceedings of the American Power Conference, Vol 40, (Illinois Institute of Technology, Technology Center, Chicago, IL)